

Exploring the Binding Site of Δ lac-Acetogenin in Bovine Heart Mitochondrial NADH–Ubiquinone Oxidoreductase[†]

Nobuyuki Kakutani, Masatoshi Murai, Naoto Sakiyama, and Hideto Miyoshi*

Division of Applied Life Sciences, Graduate School of Agriculture, Kyoto University, Sakyo-ku, Kyoto 606-8502, Japan

Received March 26, 2010; Revised Manuscript Received May 5, 2010

ABSTRACT: Biochemical characterization of the inhibition mechanism of Δ lac-acetogenins synthesized in our laboratory indicated that they are a new type of inhibitor of bovine heart mitochondrial NADH–ubiquinone oxidoreductase (complex I) [Murai, M., et al. (2006) *Biochemistry* **45**, 9778–9787]. To identify the binding site of Δ lac-acetogenins with a photoaffinity labeling technique, we synthesized a photoreactive Δ lac-acetogenin ($[^{125}\text{I}]\text{diazirylated } \Delta\text{lac-acetogenin}$, $[^{125}\text{I}]\text{DAA}$) which has a small photoreactive diazirine group attached to a pharmacophore, the bis-THF ring moiety. Characterization of the inhibitory effects of DAA on bovine complex I revealed unique features specific to, though not completely the same as those of, the original Δ lac-acetogenin. Using $[^{125}\text{I}]\text{DAA}$, we carried out photoaffinity labeling with bovine heart submitochondrial particles. Analysis of the photo-cross-linked protein by Western blotting and immunoprecipitation revealed that $[^{125}\text{I}]\text{DAA}$ binds to the membrane subunit ND1 with high specificity. The photo-cross-linking to the ND1 subunit was suppressed by an exogenous short-chain ubiquinone (Q_2) in a concentration-dependent manner. Careful examination of the fragmentation patterns of the cross-linked ND1 generated by limited proteolysis using lysylendopeptidase, endoprotease Asp-N, or trypsin and their changes in the presence of the original Δ lac-acetogenin strongly suggested that the cross-linked residues are located at two different sites in the third matrix-side loop connecting the fifth and sixth transmembrane helices.

The proton-pumping NADH–ubiquinone oxidoreductase (complex I)¹ is the first energy-transducing enzyme of the respiratory chains of most mitochondria and many bacteria. It catalyzes the oxidation of NADH by ubiquinone, coupled to the generation of an electrochemical proton gradient across the membrane that drives energy-consuming processes such as ATP synthesis (1). Complex I is the most complicated multi-subunit enzyme in the respiratory chain; e.g., the enzyme from bovine heart mitochondria is composed of 45 different subunits with a total molecular mass of about 1 MDa (2). The crystal structure of the hydrophilic domain (peripheral arm) of complex I from *Thermus thermophilus* was solved at a resolution of 3.3 Å, revealing the subunit arrangement and the putative electron transfer pathway (3). However, information about the structural and functional features of the membrane arm, such as the

ubiquinone redox reaction, proton translocation mechanism, and mode of action of numerous specific inhibitors, is still highly limited (4–6).

A variety of inhibitors act on mitochondrial complex I at the terminal electron transfer step (7–9). Although these inhibitors are generally believed to act at the ubiquinone reduction site, there have been conflicting reports (10, 11). Earlier photoaffinity labeling studies demonstrated that rotenone, pyridaben, and fenpyroximate bind to the ND1, PSST, and ND5 subunit, respectively (12–15). Recently, we indicated that a photoreactive acetogenin mimic ($[^{125}\text{I}]\text{TDA}$, Figure 1) binds to the region of the fourth to fifth transmembrane helices (Val144–Glu192) in the ND1 subunit of bovine heart complex I (16, 17). We also revealed that a quinazoline-type inhibitor binds to the interfacial region of the ND1 (membrane domain) and 49 kDa (hydrophilic domain) subunits and that the photo-cross-linked residue in the 49 kDa subunit is located within the region Asp41–Arg63 (23 amino acids) (18). On the other hand, mutagenesis studies using the yeast *Yarrowia lipolytica* (19, 20) and *Rhodobacter capsulatus* (21) indicated that the PSST and 49 kDa subunits contribute to the inhibitor binding domain. Taken together, the results indicate that subunits PSST, 49 kDa, ND1, and ND5 construct the inhibitor binding pocket in complex I. As the contribution of the ND5 subunit is debatable (22), reinvestigation of the photoaffinity labeling may be necessary using a different photoreactive fenpyroximate derivative (15).

Acetogenins such as bullatacin (Figure 1) and rolliniastatin-1 are among the most potent inhibitors of bovine heart mitochondrial complex I (7–9). Although they have little structural similarity with classical complex I inhibitors such as piericidin A and rotenone, acetogenins may share a common binding domain with the other inhibitors (16, 23). On the basis of structure–activity

[†]This work was supported in part by a Grant-in-Aid for Scientific Research from the Japan Society for the Promotion of Science (Grant 20380068 to H.M.) and a Grant-in-Aid for Young Scientists (Grant 21880024 to M.M.).

*To whom correspondence should be addressed: e-mail, miyoshi@kajs.kyoto-u.ac.jp; tel, +81-75-753-6119; fax, +81-75-753-6408.

¹Abbreviations: 6-aminoquinazoline, 6-amino-4-(4-*tert*-butylphenethylamino)quinazoline; BN-PAGE, blue-native polyacrylamide gel electrophoresis; CBB, Coomassie brilliant blue; complex I, mitochondrial proton-pumping NADH–ubiquinone oxidoreductase; DAA, diazirinylated Δ lac-acetogenin; $[^{125}\text{I}]\text{DAA}$, $[^{125}\text{I}]$ -labeled DAA; DDM, *n*-dodecyl β -D-maltoside; IC_{50} , the molar concentration (nM) needed to reduce the control NADH oxidase activity in SMP by half; LHON, Leber's hereditary optic neuropathy; MELAS, mitochondrial encephalopathy, lactic acidosis, and stroke-like episodes; MALDI-TOF, matrix-assisted laser desorption ionization time of flight; MS, mass spectrometry; PVDF, polyvinylidene fluoride; SDS–PAGE, sodium dodecyl sulfate–polyacrylamide gel electrophoresis; SMP, submitochondrial particles; $[^{125}\text{I}]\text{TDA}$, $[^{125}\text{I}]$ -labeled (trifluoromethyl)phenyldiaziriny-lacetogenin; THF, tetrahydrofuran.

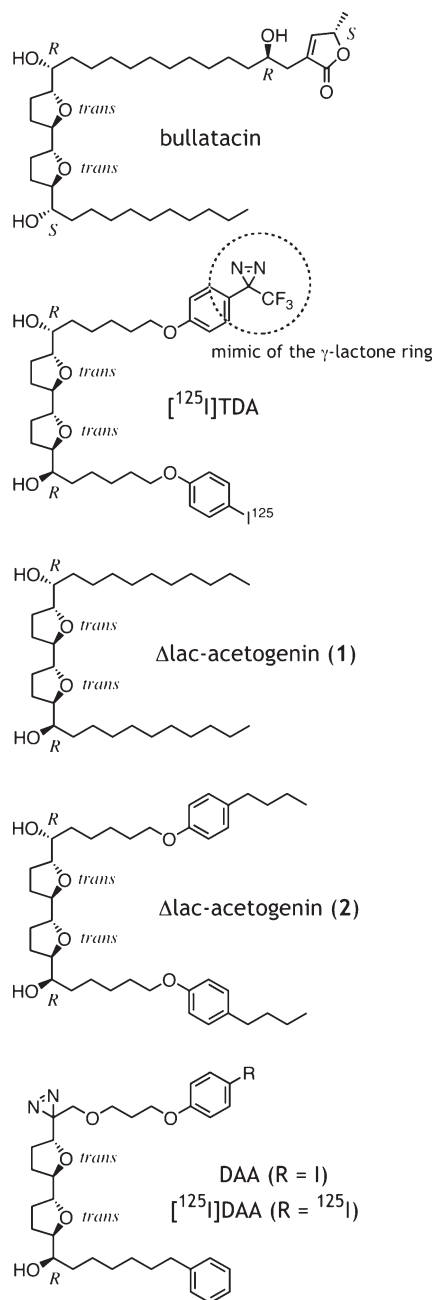


FIGURE 1: Structures of the test compounds used in the present study.

relationship for a series of acetogenins, we disclosed important structural factors required for the inhibitory action (24–28). In the course of modifying natural acetogenins, we deleted a γ -lactone ring, a structural feature common to a large number of natural acetogenins, from the mother skeleton and named the resultant derivatives “ Δ lac-acetogenins” (29). Unexpectedly, Δ lac-acetogenins (e.g., compounds **1** and **2**, Figure 1) retained strong inhibitory activity against bovine complex I at the nanomolar level. Detailed biochemical characterization revealed the Δ lac-acetogenins to be a new type of complex I inhibitor, as summarized below (16, 30, 31). First, the most characteristic feature of Δ lac-acetogenins is that they induce superoxide production from bovine heart complex I, regardless of whether endogenous or exogenous ubiquinone is used, at much lower rates than do classical inhibitors (30, 31). Second, their inhibitory effect on ubiquinol–NAD⁺ oxidoreductase activity (reverse electron transfer) is significantly weaker than that on NADH oxidase activity (forward electron transfer); i.e., they are direction-specific

inhibitors (16, 31). Third, unlike traditional inhibitors such as rotenone and piericidin A, Δ lac-acetogenins do not prevent the specific photo-cross-linking of the ND1 subunit by [¹²⁵I]-TDA (16). Thus, the inhibition mechanism of Δ lac-acetogenins is quite different from that of traditional inhibitors. In view of the proposed dynamic function of the membrane domain (32–35), it is not strange that there are diverse chemicals that disturb this function differently depending on their structural nature.

Considering the unusual effects of Δ lac-acetogenins, further exploration of their inhibitory mechanism including the identification of their binding site would provide valuable insights into the terminal electron transfer step of complex I. We here synthesized a photoreactive Δ lac-acetogenin mimic ([¹²⁵I]*diazinylated* Δ lac-acetogenin, [¹²⁵I]DAA, Figure 1), which has a small photolabile diazirine group attached to the pharmacophore, i.e., bistetrahydrofuran (THF) ring moiety, and carried out photoaffinity labeling with bovine heart submitochondrial particles (SMP). The results revealed that the binding site of [¹²⁵I]DAA resides in the ND1 subunit of the membrane domain. Limited proteolysis of the ND1 cross-linked by [¹²⁵I]DAA using various proteases and changes in the presence of original Δ lac-acetogenin indicated that the hydrophilic bis-THF ring moiety binds at two different sites in the third matrix side loop connecting the fifth and sixth transmembrane helices.

EXPERIMENTAL PROCEDURES

Materials. Bullatacin and piericidin A were kindly provided by Drs. J. L. McLaughlin (Purdue University, West Lafayette, IN) and S. Yoshida (The Institute of Physical and Chemical Research, Saitama, Japan), respectively. The rabbit anti-ND1 antibody was a generous gift from Dr. T. Yagi (The Scripps Research Institute, La Jolla, CA). Representative Δ lac-acetogenins (**1** and **2**) and 6-amino-4-(4-*tert*-butylphenethylamino)quinazoline (6-aminoquinazoline) were the same samples used previously (31, 36). Protein standards (Precision Plus protein standards and Kaleidoscope polypeptide standards) for SDS–PAGE were purchased from Bio-Rad (Hercules, CA). [¹²⁵I]NaI was purchased from Perkin-Elmer (Waltham, MA). Other reagents were all of analytical grade.

Synthesis of DAA and [¹²⁵I]DAA. The procedures used to synthesize the photoreactive DAA and its ¹²⁵I-labeled derivative ([¹²⁵I]DAA) are described in the Supporting Information. The radiochemical yield from the initial [¹²⁵I]NaI was 68%, and the specific radioactivity was ~2000 Ci/mmol. Radiochemical purity was examined by HPLC and determined to be over 99%.

Preparation of Bovine Submitochondrial Particles and Enzyme Assays. Submitochondrial particles (SMP) were prepared from isolated bovine heart mitochondria (37) by the method of Matsuno-Yagi and Hatefi (38) and stored in a buffer containing 250 mM sucrose and 10 mM Tris-HCl (pH 7.4) at –80 °C until use. NADH oxidase activity and reverse electron transfer (ubiquinol–NAD⁺ oxidoreductase activity) in SMP were measured according to the procedures described previously (16, 39). The amount of superoxide generated from complex I in SMP was measured using (+)-epinephrine (bitartrate salt) as described previously (16, 40).

Photoaffinity Labeling of SMP. Bovine SMP (0.6–1.0 mg of protein/mL, 100 μ L in a 1.5 mL tube) were incubated with [¹²⁵I]DAA (6–250 nM) in buffer containing 250 mM sucrose, 1 mM MgCl₂, and 50 mM KP_i (pH 7.4) for 10 min at room temperature. Then, the samples were photoirradiated for 10 min with a long-wavelength UV lamp (Black Ray model B-100A;

UVP, Upland, CA) on ice at a distance of 10 cm from the light source. When competition was examined, a competitor was added and incubated for 10 min at room temperature prior to the treatment with [125 I]DAA.

Electrophoresis. Sodium dodecyl sulfate–polyacrylamide gel electrophoresis (SDS–PAGE) was performed according to Laemmli (41). Briefly, photoaffinity-labeled samples were added to 4 \times Laemmli's sample buffer and incubated at 35 °C for 1 h to avoid protein aggregation. These denatured samples were separated on 12.5% Laemmli's gels. After the electrophoresis, the gels were stained with CBB R-250, dried, and exposed to an imaging plate (BAS-MS2040; Fuji Film, Tokyo, Japan). The migration patterns of radiolabeled proteins were analyzed and visualized with a bio-imaging analyzer FLA-5100 (Fuji Film). The radioactivity of each band was quantified from the digitalized data using "Multi Gauge" software (Fuji Film) or directly from the dried gel slices using a γ -counting system (COBLA II; Packard).

Analytical blue-native (BN) PAGE (analytical scale) was performed using the native PAGE Novex Bis-tris gel system with a 4–16% precast gel (Invitrogen, Carlsbad, CA). The SMP photo-cross-linked by [125 I]DAA were solubilized with 1% (w/v) DDM for 1 h on ice and mixed with 4 \times sample buffer and 5% (w/v) Serva blue G (CBB G-250). Electrophoresis was performed at a voltage of 150 V with a limited current of 15 mA/gel in a cold room. After the electrophoresis, the complex I band was identified by staining "in-gel" activity with the NADH/NBT system (42) and autoradiographed as described above.

Preparative BN-PAGE was performed using a 6% isocratic hand-cast gel (160 \times 180 \times 2 mm) (43). Complex I was isolated by electroelution in an elution buffer containing 25 mM tricine and 7.5 mM Bis-tris (adjusted to pH 7.0 with HCl) using a Centrilmotor equipped with a Centricon YM-100 (Millipore, Billerica, MA). The complex I obtained was stored at –80 °C until used.

Immunochemical Analysis. The mobility of the ND1 subunit on the SDS gel was profiled by Western blotting as described previously (44). Electrophoresed mitochondrial protein or complex I was transferred onto a PVDF membrane (Immunoblot PVDF membrane, 0.2 μ m; Bio-Rad, Hercules, CA) in a buffer containing 10 mM NaHCO₃, 3 mM NaCO₃, and 0.025% (w/v) SDS overnight at 35 V (100 mA) in a cold room. The blotted membrane was blocked with 1% gelatin in Tween TBS (0.9% NaCl, 0.05% Tween 20, and 10 mM Tris-HCl (pH 7.4)) for 1 h at room temperature. The blocked PVDF membrane was probed with the rabbit anti-bovine ND1 antibody (2000 \times dilution) for 1 h at room temperature and then incubated for another 1 h with alkaline phosphatase (AP) conjugated secondary antibodies (Daiichi Pure Chemicals, Tokyo, Japan) at room temperature. The treated membrane was washed with Tween TBS (10 min \times 3 times) and developed with NBT/BCIP chromogenic substrates (AP color development kit; Bio-Rad).

Immunoprecipitation of the ND1 subunit was carried out according to the procedures described previously using the electroeluted complex I as a starting material (14, 16). The electroeluted complex I was denatured with 1.25% SDS (60 μ L) and diluted with binding buffer (240 μ L) containing 1.25% Triton X-100, 190 mM NaCl, 6 mM EDTA, 0.1 mM PMSF, and 60 mM Tris-HCl (pH 7.4). The rabbit anti-bovine ND1 antiserum (5 μ L) was added to the mixture (300 μ L) and incubated overnight in a cold room. Protein A–Sepharose 4 (30 μ L slurry, equilibrated with the binding buffer; GE Healthcare, U.K.) was added and rotated for 2 h at room temperature. The suspension was washed four times (0.8 mL) with a washing buffer containing 0.1%

Triton X-100, 0.02% SDS, 150 mM NaCl, 5 mM EDTA, and 50 mM Tris-HCl (pH 7.4) and once (0.8 mL) with a washing buffer without detergents. The captured ND1 on the resin was released by treating with 1 \times Laemmli's buffer and subjected to SDS–PAGE and autoradiography.

Isolation and Limited Proteolysis of the ND1 Subunit. For limited proteolysis of the ND1 subunit, the SMP cross-linked by [125 I]DAA were partially isolated by SDS–PAGE on 12.5% Laemmli's gel according to the previous procedure (17). Limited proteolysis was performed using lysylendopeptidase (Lys-C; Wako Pure Chemicals, Osaka, Japan), endoprotease Asp-N (Roche Applied Science, Penzberg, Germany), or trypsin (Promega, Madison, WI) in 20 mM Tris-HCl buffer (pH 9.0, containing 0.1% SDS), 50 mM phosphate buffer (pH 8.5, containing 0.01% SDS), or ammonium bicarbonate buffer (pH 7.8, containing 0.01% SDS), respectively (17). The digestion was continued overnight at 37 °C. The digestion was quenched with 4 \times sample buffer, and the sample was further analyzed by tricine/SDS–PAGE (16.5% T/6% C) (45).

Sequence Analysis and Topology Prediction of the ND1 Subunit. The number of transmembrane helices and membrane topology of the bovine ND1 subunit were predicted as described previously (17). The mobility shifts of enzymatic digests on tricine gel were compared with theoretical digests of the published protein sequences of the bovine ND1 (Swiss Prot: P03887) using Peptide Mass (<http://expasy.org/tools/peptide-mass.html>).

RESULTS

Design Concept for a Photoreactive Δ lac-Acetogenin. When synthesizing a probe for photoaffinity labeling, particular attention should be given to avoid significant loss of the inherent biological activity of the inhibitor due to the introduction of a photolabile cross-linking group. Therefore, the identification of critical structural factors of the inhibitor is necessary. Previous structure–activity studies concerning numerous Δ lac-acetogenins revealed several important structural factors required for a potent inhibitory effect. First, the number of carbon atoms deciding the hydrophobicity of the alkyl side chains remarkably influences the inhibitory effect (29). Second, the balance of the hydrophobicity of the two chains attached to the C₂-symmetric bis-THF portion is also an important factor: the greater the loss of this balance, the weaker the inhibitory effect (46). Third, deletion of both hydroxyl groups results in an almost complete loss of activity, but the presence of one of the two hydroxyl groups can sustain fairly strong activity (30). Fourth, the stereochemistry around the hydroxylated bis-THF ring moiety significantly influences the inhibitory effect (47); the *R*-configuration at all chiral centers as in compounds **1** and **2** is the most favorable for the inhibition. All together, it is concluded that the hydroxylated bis-THF ring moiety is the only critical structural unit of Δ lac-acetogenins and no specific functional group is required in the alkyl tail moieties.

Based on the results of structure–activity studies, there were two choices as to where a photolabile group should be attached: the alkyl tails and the bis-THF ring moiety. From a synthetic point of view, the former choice is much easier since no specific structure in the tails, except large hydrophobicity, is required for the activity. However, we did not choose this option because (i) the region of the enzyme cross-linked by the photolabile group attached to the *unessential* moiety of the inhibitor would not be responsible for critical interaction with the inhibitor and (ii) the alkyl tails may be too flexible to fix the position of the photolabile

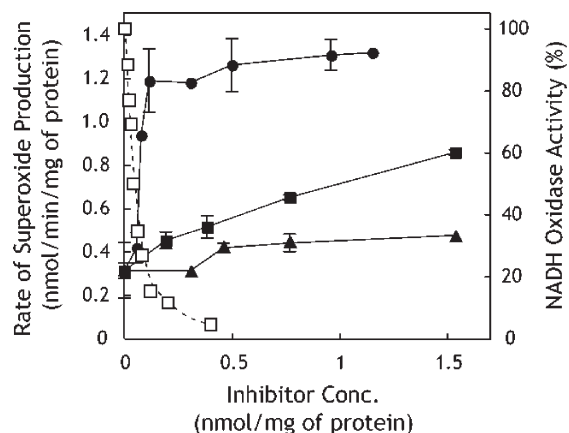


FIGURE 2: Correlation between the rate of superoxide production and the inhibition of the NADH oxidase activity in SMP. Superoxide production: bullatacin (closed circles), **2** (closed triangles), and DAA (closed squares). Inhibition of the NADH oxidase activity: DAA (open squares). Bars show means \pm SD of three independent measurements.

group in the enzyme. Consequently, to explore the critical interaction between the inhibitor and the enzyme, we decided to introduce a small diazirine group adjacent to the essential bis-THF ring (DAA, Figure 1). Extensive hydrophobicity of the tail moieties was attained by introducing two benzene rings, one of which bears a radioisotope tag (^{125}I).

Characterization of Inhibitory Effect of DAA. To examine whether DAA is a possible candidate for a photoaffinity probe of Δ lac-acetogenins, we characterized its inhibitory effect on bovine complex I. First, the inhibitory effect of DAA was examined with the NADH oxidase activity in SMP (30 μg of protein/mL). The IC_{50} values of DAA, **2**, and bullatacin were $1.2 (\pm 0.10)$, $0.90 (\pm 0.11)$, and $0.85 (\pm 0.07)$ nM, respectively. This result indicates that DAA retains strong inhibitory activity irrespective of the displacement of a hydroxy group attached to the bis-THF ring with a diazirine group.

Next, we measured the superoxide production from complex I induced by DAA in the NADH oxidase assay using bullatacin and **2** as references (Figure 2). It should be noted that complete inhibition of the electron transfer activity by these inhibitors was attained below ~ 0.5 nmol/mg of protein under the experimental conditions, as shown in Figure 2 taking DAA as an example. The level of superoxide production induced by **2** was markedly lower than that induced by bullatacin throughout the range of concentrations examined, as reported previously (31). DAA also induced much less superoxide than bullatacin over the concentration range achieving specific inhibition of the electron transfer activity. However, the level of superoxide production increased gradually with an increase in the inhibitor concentration far beyond the level completely inhibiting the electron transfer event.

Finally, we compared the inhibitory activity of DAA between the forward and the reverse electron transfer events. The IC_{50} values (picomoles of inhibitor per milligram of protein) for the forward and reverse electron transfer activity and the ratio of IC_{50} (reverse) to IC_{50} (forward) are listed in Table 1, with bullatacin, rotenone, and **2** as references. Compared to classical inhibitors, DAA inhibited the reverse electron transfer more weakly than the forward event, as observed with **2** (31).

With all things combined, we conclude that the inhibitory action of DAA is not identical to that of original Δ lac-acetogenins due to the structural modification; nevertheless, DAA actually has unique inhibitory effects specific to the Δ lac-acetogenins.

Table 1: Inhibitory Effects on the Forward and Reverse Electron Transfer Activities

inhibitor	IC_{50} values (pmol of inhibitor/mg of protein) ^a		$\text{IC}_{50}(\text{R})/\text{IC}_{50}(\text{F})^b$
	forward electron transfer	reverse electron transfer	
rotenone ^c	130 ± 14	62 ± 8.0	0.48
bullatacin	28 ± 3.7	28 ± 4.4	0.93
pipecidin A ^c	81 ± 7.1	48 ± 4.3	0.59
compound 2	30 ± 2.3	180 ± 21	6.0
DAA	39 ± 3.3	317 ± 25	8.1

^aValues are the mean \pm SD of three independent experiments. ^bThe ratio of IC_{50} (reverse) to IC_{50} (forward). ^cFrom ref 31.

Therefore, DAA can be regarded as a candidate for a photoaffinity probe directed toward identification of the binding site of Δ lac-acetogenins.

Photoaffinity Labeling of Bovine SMP Using [^{125}I]DAA.

For the photoaffinity labeling experiment, SMP were used to ensure the intactness of complex I. When SMP (0.6 mg of protein/mL) were UV-irradiated in the presence of 6 nM [^{125}I]DAA, which causes 5–15% inhibition of NADH oxidase activity, only one cross-linked protein, with an apparent molecular mass of approximately 30 kDa, was found on the SDS gel (Figure 3A). We next examined the correlation between the incorporation of the radioactivity into the 30 kDa protein and the inhibition of the NADH oxidase activity. Even at higher concentrations of [^{125}I]DAA up to 640 nM, the radioactivity in other regions on the SDS gel was less than 5% of that in the 30 kDa region. As shown in Supporting Information Figure S1, the incorporation of the radioactivity into the 30 kDa protein was not saturated at high concentrations far beyond the level completely inhibiting the electron transfer activity. This phenomenon may be related to the concentration dependency observed for the superoxide production induced by DAA (Figure 2), as described later.

Identification of the Cross-Linked 30 kDa Protein. The 30 kDa protein cross-linked by [^{125}I]DAA was identified as described previously (16). The [^{125}I]DAA-labeled SMP were subjected to blue-native (BN) PAGE and resolved into five oxidative phosphorylation enzyme complexes (Figure 3B, left). The complex I band was identified by the activity staining using a NADH–NBT system (Figure 3B, center). Major radioactivity was detected in this band (Figure 3C, right).

Next, the radiolabeled complex I was isolated by electroelution and subjected to SDS–PAGE for further separation. As shown in Figure 3C (center), we detected major radioactivity in an ~ 30 kDa protein, indicating that the [^{125}I]DAA-labeled protein is a component of complex I. When samples were boiled for 10 min prior to the SDS–PAGE analysis, extensive aggregation of the protein took place (Figure 3C, center). This observation along with the apparent molecular mass of the protein strongly suggests that this protein is the ND1 subunit in the membrane domain. To verify this, we carried out Western blotting (Figure 3C, right) and immunoprecipitation (Figure 3D) using the anti-bovine ND1 antibody. The results clearly indicated that the radiolabeled protein is the ND1 subunit.

Suppression of the Specific Labeling of ND1 by Other Complex I Inhibitors. We examined the effect of various complex I inhibitors, including an original Δ lac-acetogenin (**2**), on the specific cross-linking of the ND1 subunit by [^{125}I]DAA. As shown in Figure 4A, classical inhibitors such as bullatacin and rotenone suppressed the cross-linking at a concentration ranging

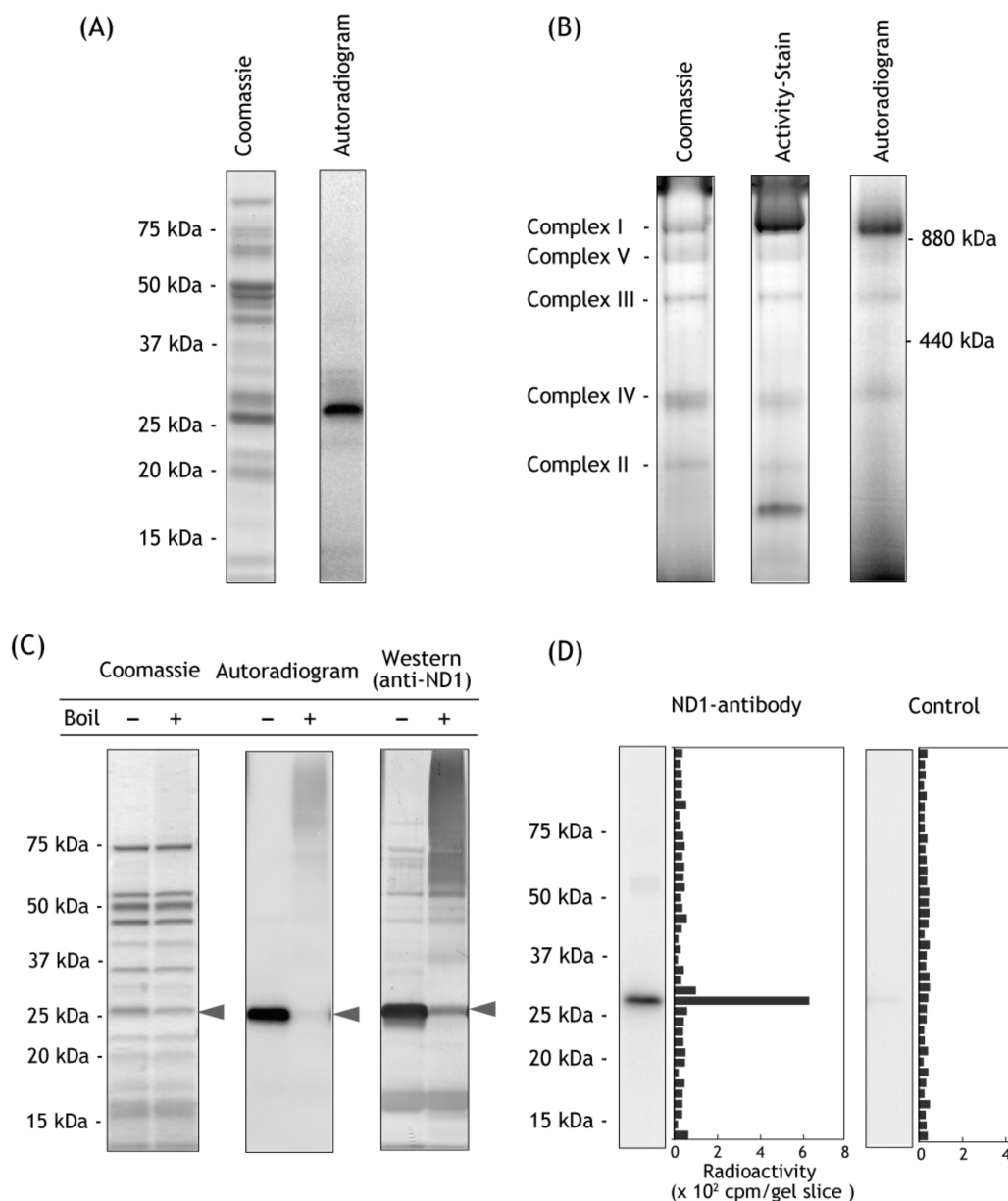


FIGURE 3: Photoaffinity labeling of bovine SMP and characterization of the 30 kDa protein cross-linked by [¹²⁵I]DAA. (A) Bovine SMP (0.6 mg of protein/mL) were photo-cross-linked by 6 nM [¹²⁵I]DAA and analyzed by SDS-PAGE on 12.5% Laemmli's gel (24 and 12 μ g of protein per lane for CBB and autoradiography, respectively). (B) SMP (1.5 mg of protein/mL) were photo-cross-linked by 10 nM [¹²⁵I]DAA. The labeled SMP were solubilized with 1% (w/v) DDM and resolved on a 4–15% BN gel according to the Experimental Procedures, stained with NBT/NADH, and autoradiographed. (C) Complex I photo-cross-linked by [¹²⁵I]DAA (15 nM [¹²⁵I]DAA at 1.5 mg of protein/mL) was isolated from the preparative BN gel by electroelution. The isolated complex I was analyzed by SDS-PAGE on 12.5% Laemmli's gel (equivalent to 50 μ g of SMP protein per lane), followed by CBB staining (left), autoradiography (center), and Western blotting using the ND1 antibody (right). In order to examine its stability, the samples were heated at 95 °C for 10 min. (D) For the identification of the 30 kDa protein cross-linked by [¹²⁵I]DAA, the isolated complex I was subjected to immunoprecipitation with the bovine ND1 antibody as described in the Experimental Procedures.

from 30 to 3000 nM (5–500-fold excess of [¹²⁵I]DAA). 6-Aminoquinazoline and piericidin A also completely suppressed the cross-linking at 3000 nM (data not shown). It is worth noting that a 50-fold excess of bullatacin, a reversible inhibitor forming no covalent bond with the enzyme, completely blocked the cross-linking. This suppression was the most pronounced effect among the photoaffinity labeling studies performed in our laboratory (16–18). Unexpectedly, 30–40% of the radioactivity was retained in the ND1 subunit even in the presence of a 500-fold excess of **2**, suggesting that there is an additional binding site(s) for DAA, which Δ lac-acetogenin cannot access.

Suppression of the Specific Labeling of ND1 by Exogenous Quinone. Recently, we showed that an excess amount of short-chain ubiquinones such as ubiquinone-2 (Q₂) suppressed the

photo-cross-linking of the ND1 subunit by an acetogenin mimic, [¹²⁵I]TDA, in a concentration-dependent manner (17). Among early photoaffinity labeling studies using photoreactive inhibitors or quinones (10–15, 18, 23), the paper was the first to report direct evidence that an inhibitor and ubiquinone competitively bind to the enzyme. It should be noted that competition experiments between strong inhibitors and exogenous short-chain ubiquinones would be difficult since the affinity of the two ligands differs too greatly (by about 3 orders of magnitude) to examine efficient competitive behavior over a limited concentration range.

We examined the competition between [¹²⁵I]DAA and Q₂ by determining the suppressive effect of Q₂ on the cross-linking of the ND1 subunit by [¹²⁵I]DAA. Actually, Q₂ suppressed the

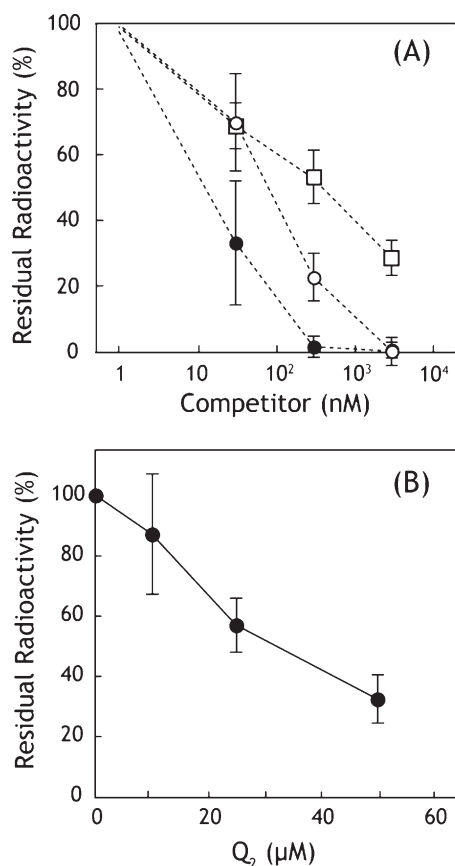


FIGURE 4: Effect of various complex I inhibitors or Q₂ on the specific cross-linking of [¹²⁵I]DAA. (A) SMP (0.6 mg of protein/mL) were photo-cross-linked by 6 nM [¹²⁵I]DAA in the presence of a given concentration of complex I inhibitors. The labeled SMP were separated on 12.5% Laemmli's gel, and the residual radioactivity in the ND1 subunit was measured: bullatacin (closed circles), rotenone (open circles), and compound 2 (open squares). The average control radioactivity in the ND1 subunit is 1200 cpm. (B) SMP (0.6 mg of protein/mL) were photo-cross-linked by 6 nM [¹²⁵I]DAA in the presence of a given concentration of Q₂. Data are the mean of three independent experiments \pm SD.

cross-linking in a concentration-dependent manner (Figure 4B). Complete suppression was not observed in the concentration range studied. The use of higher concentrations of Q₂ than those examined in Figure 4B was impractical because of the solubility limit. It may be mentioned that photo-cross-linking of the 49 kDa and ND1 subunits by a quinazoline-type inhibitor ([¹²⁵I]AzQ) was suppressed only by \sim 10% in the presence of 30 μ M Q₂ under the same experimental conditions (18), indicating that the suppression of [¹²⁵I]DAA binding is not due to nonspecific perturbation of the enzyme (or the membrane) structure by hydrophobic Q₂.

Analysis of the Cross-Linked Region of [¹²⁵I]DAA in the ND1 Subunit. We tried to identify the binding site of [¹²⁵I]DAA in the ND1 subunit by analyzing fragmentation patterns of the cross-linked ND1 generated by limited proteolysis using different proteases. The digestion of the cross-linked ND1 by Lys-C gave a single radioactive band with an apparent molecular mass of \sim 15 kDa on a tricine gel (Figure 5, left). Careful analysis of the sites cleavable by Lys-C (Figure 6A) provided the sequence Tyr127–Lys262 with a calculated molecular mass of 15.1 kDa, which covers the fourth to seventh transmembrane helices.

The Asp-N treatment of the cross-linked ND1 subunit gave two radioactive digests with apparent molecular masses of \sim 17 and \sim 9 kDa at a frequency of \sim 3:2 (Figure 5, center). Taking into consideration the theoretical sites of cleavage by Asp-N

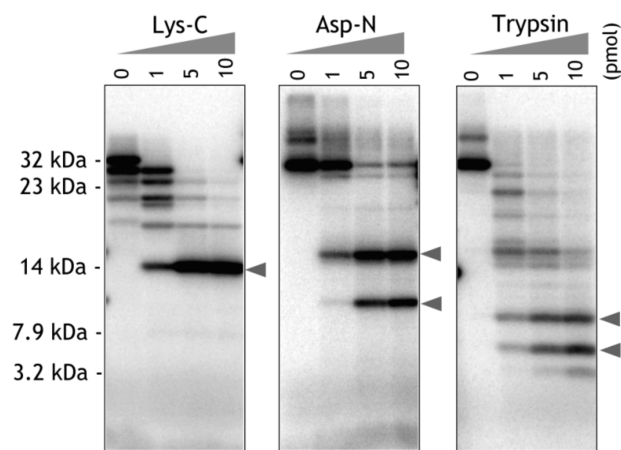


FIGURE 5: Proteolytic analysis of the ND1 subunit cross-linked by [¹²⁵I]DAA. The cross-linked ND1 was partially purified by SDS-PAGE and electroelution as described in the Experimental Procedures. The isolated ND1 subunit was digested by lysylendopeptidase (Lys-C, left), endoprotease Asp-N (center), or trypsin (right). The digestion was quenched by the addition of 4 \times sample buffer, followed by tricine/SDS-PAGE (16.5% T/6% C). The amounts of proteases added are indicated on the top of each autoradiogram. Data shown are representative of three independent experiments.

(Figure 6A) along with the result of the Lys-C digestion, these fragments must be Asp51–Phe198 (covering the second to fifth transmembrane helices, 16.3 kDa) and Asp199–Tyr282 (covering the sixth to seventh transmembrane helices, 9.7 kDa). This result indicates that [¹²⁵I]DAA has two different cross-linking sites in the ND1 subunit. It is unclear whether the radioactivity frequency of the two bands (\sim 3:2) accurately reflects the ratio of the occupancy of the two sites by [¹²⁵I]DAA because photo-cross-linking yields are not necessarily identical at the two sites.

The tricine/SDS-PAGE analysis of the tryptic digests of the cross-linked ND1 subunit also gave two radioactive bands with apparent molecular masses of \sim 9 and \sim 6 kDa at a frequency of \sim 1:1 (Figure 5, right), though the radioactivity in the two bands was much lower than that in the bands generated by Asp-N treatment. From the theoretical sites of cleavage by trypsin (Figure 6A) along with the results of Lys-C and Asp-N treatment, these fragments must be Ala196–Lys262 (covering the sixth to seventh transmembrane helices, 7.5 kDa) and Ala135–Arg195 (covering the fourth to fifth transmembrane helices, 6.8 kDa).

To pinpoint the amino acid residue(s) cross-linked by [¹²⁵I]DAA, we carried out MALDI-TOF MS analysis of the tryptic digests of the ND1 subunit. However, the region covering the fourth to seventh transmembrane helices was not detected because of low sequence coverage (\sim 15%). Similar low coverage of the hydrophobic ND1 subunit was reported in previous mass spectrometric studies of this subunit (18, 48).

Effect of Δ lac-Acetogenin on the Binding of [¹²⁵I]DAA to the Different Sites. The above results strongly suggested that [¹²⁵I]DAA has two different binding sites in the region covering the fourth to seventh transmembrane helices of the ND1 subunit. For convenience, the putative two sites located in the Tyr127–Phe198 and Asp199–Lys262 regions, the common regions generated by Asp-N and Lys-C treatment, are termed “site A” and “site B”, respectively (Figure 6B). It is critical to establish whether both sites are responsible for the binding of a bis-THF ring moiety of the original Δ lac-acetogenins. As \sim 40% of the radioactivity was retained in the ND1 subunit when the photo-cross-linking

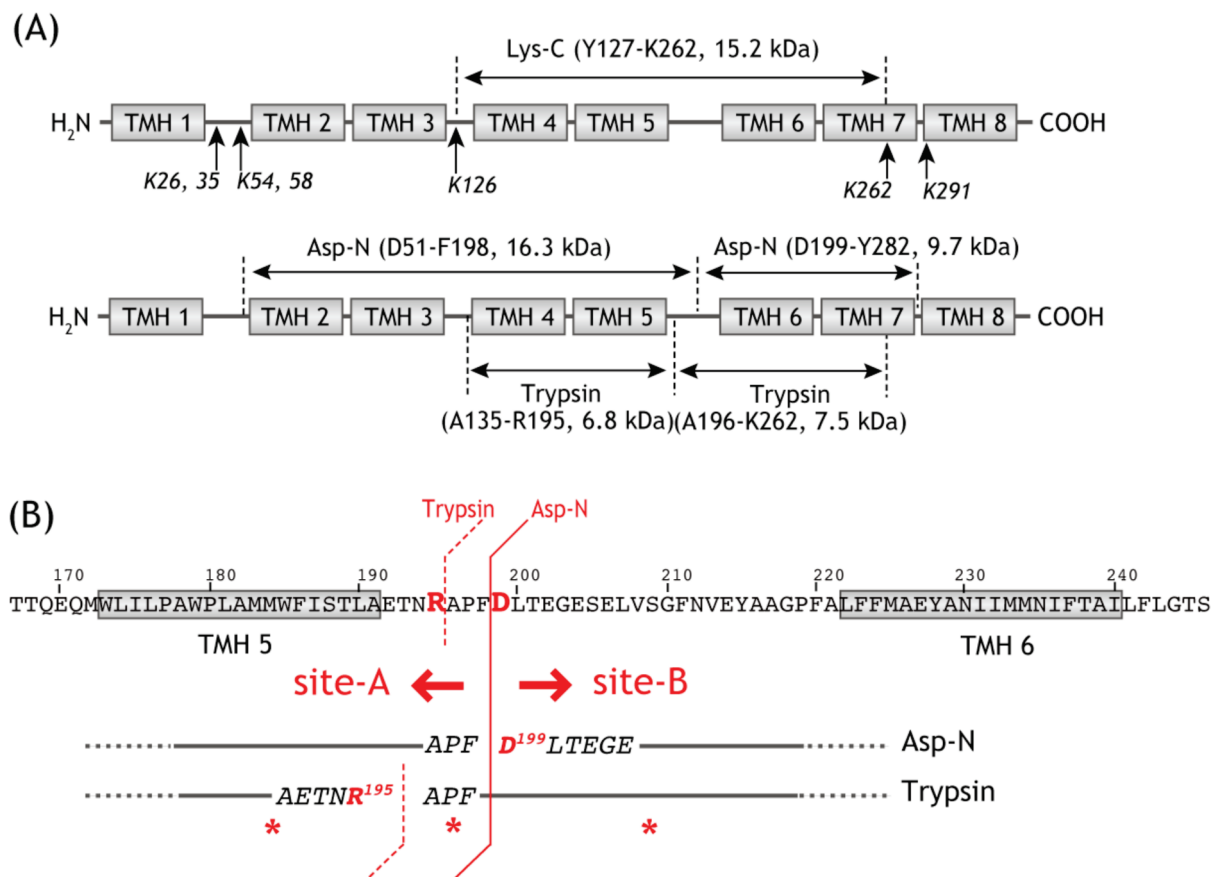


FIGURE 6: A digestion map of the ND1 subunit cross-linked by [¹²⁵I]DAA. (A) A schematic representation of Lys-C, Asp-N, or tryptic digestion of the ND1 subunit. The numbers of transmembrane helices and its position of the ND1 subunit were predicted according to the previous method (17). The residue numbers refer to the mature sequence of the bovine ND1 subunit (P03887). (B) Conceptual representation of site A and site B.

was carried out in the presence of a 500-fold excess of **2** (Figure 4A), we examined the residual radioactivity in the two fragments generated by Asp-N or trypsin in the presence of **2**.

SMP (0.6 mg of protein/mL) were cross-linked with 15 nM [¹²⁵I]DAA in the presence of 750 nM or 3 μ M **2**, digested by Asp-N, and subjected to a tricine/SDS-PAGE analysis. As shown in Figure 7A, radioactivity was incorporated into the fragment Asp51–Phe198 containing site A, but its incorporation into the fragment Asp199–Tyr282 containing site B was blocked by **2** in a concentration-dependent manner. A 200-fold excess of **2** completely blocked the cross-linking to site B. This result indicates that the original Δ lac-acetogenin predominantly binds to site B.

Digestion with trypsin provided a result different from that obtained with the Asp-N. Namely, the incorporation of radioactivity into the fragment A196–K262 containing site B was not completely blocked even by a 200-fold excess of **2**, though the level of radioactivity was slightly reduced compared to that in the fragment Ala135–Arg195 (Figure 7B). To explain these contradictory results, we propose that there are two cross-linked residues at site A: one on the N-terminal side of Arg195 and the other between Ala196 and Phe198, as shown by asterisks in Figure 6B. In light of the inhibition mechanism of natural acetogenins, we will discuss this point later.

We also examined the effect of Q₂ on the cross-linking of the two fragments generated by Asp-N. SMP (0.6 mg of protein/mL) were cross-linked with 15 nM [¹²⁵I]DAA in the presence of 125 μ M Q₂, digested by Asp-N, and subjected to a tricine/SDS-PAGE analysis. Interestingly, the cross-linking to the fragment Asp199–Tyr282 was predominantly blocked by Q₂ (Figure 7C).

DISCUSSION

The inhibitory mechanism of Δ lac-acetogenins is different from that of numerous classical inhibitors of complex I (16, 29–31). Nevertheless, the photoaffinity labeling performed in the present work revealed that the binding site of Δ lac-acetogenin resides in the membrane subunit ND1, which also accommodates classical inhibitors such as rotenone (12, 13), natural acetogenin (16, 17), and quinazoline (18). The ND1 subunit is one of seven mitochondrially encoded hydrophobic subunits of the membrane arm of complex I and a mutational hot spot for mitochondrial diseases like LHON (49) and MELAS (50), underscoring its physiological role. This subunit has been assumed to play key roles in assembly/communication between the peripheral and membrane domains (51). In support of this notion, a series of photoaffinity labeling studies carried out in our laboratory indicated that the ND1 is one of the subunits which construct a large inhibitor binding domain in bovine heart complex I (16–18).

Careful examination of the fragmentation patterns of the cross-linked ND1 generated by various proteases indicated that the hydroxylated bis-THF moiety of [¹²⁵I]DAA binds to two different regions, Tyr127–Phe198 (containing site A) and Asp199–Lys262 (containing site B), and that the presence of an excess amount of original Δ lac-acetogenin (**2**) predominantly blocks the cross-linking of the latter region. To predict the binding sites of the bis-THF ring moiety in these regions, information from structure–activity studies for numerous Δ lac-acetogenins may be helpful. We previously demonstrated that a

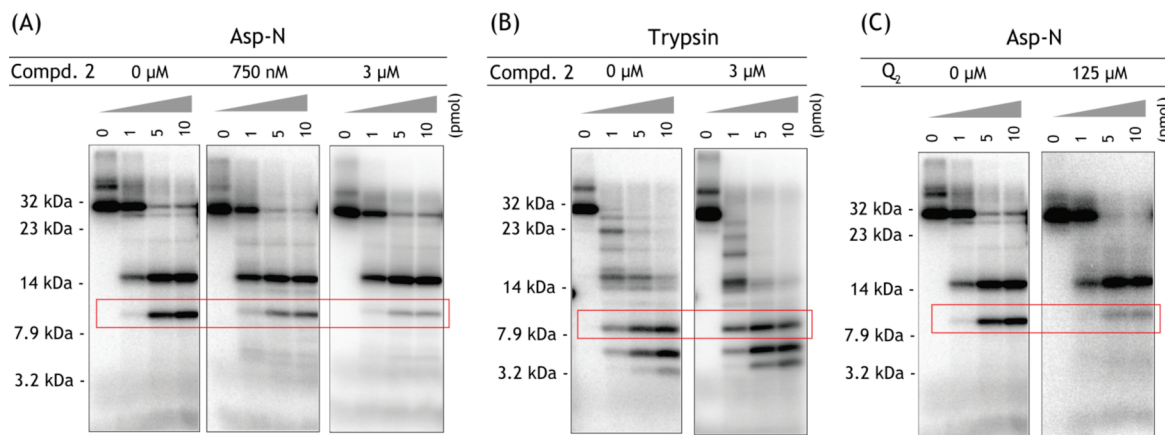


FIGURE 7: Comparison of the digestion patterns of the cross-linked ND1 subunit in the presence or absence of Δ lac-acetogenin (**2**) or Q_2 . SMP (1.5 mg of protein/mL) were cross-linked by 15 nM [125 I]DAA in the presence of **2** [750 nM (50-fold) or 3.0 μ M (200-fold)] or Q_2 [125 μ M (8300-fold)]. The cross-linked ND1 was partially purified by SDS–PAGE and subjected to Asp–N or tryptic digestion, followed by tricine/SDS–PAGE as shown in Figure 5. (A, B) Effect of **2** on the Asp–N and tryptic digests, respectively, of the cross-linked ND1. (C) Effect of Q_2 on the Asp–N digests of ND1. For comparison, the radioactivity of each lane was set to be identical (800 cpm per lane). The Asp–N digest (Asp199–Tyr282, 9.7 kDa) and the tryptic digest (Ala196–Lys262, 7.5 kDa) are surrounded by red rectangles. Data shown are representative of three independent experiments.

balance of the hydrophobicity of the two tails is critical for strong activity: the greater the loss of this balance, the weaker the inhibitory effect (30, 46). It is reasonable to consider that the hydrophilic bis-THF ring moiety of these amphiphilic inhibitors resides at or close to the polar membrane surface. The hydrophobic tails may decide the precise location of the bis-THF ring in the membrane surface area by anchoring into the hydrophobic enzyme or membrane environment. Therefore, the hydrophilic bis-THF ring of DAA may reside in the third matrix side loop, which is highly enriched in invariantly conserved charged residues (51, 52), as illustrated in Figure 8. Taking the results of the competition test using **2** into consideration, the bis-THF ring moiety of original Δ lac-acetogenins may bind predominantly to site B.

Neither the extent of the photo-cross-linking of ND1 by [125 I]DAA nor the production of superoxide induced by DAA was saturated at up to about 1.5 nmol of inhibitor/mg of protein, concentrations far beyond that required for complete inhibition of the electron transfer activity. However, it should be realized that the labeling at high concentrations involves high specificity in the binding and reaction with a single subunit (ND1) within a mixture of many proteins in SMP. To explain these observations, we speculate that the binding of DAA to site B induces just a little superoxide, as observed for **2**, but the binding to site A, which increases with an increase in the DAA concentration, results in enhanced superoxide production. It is difficult at present to know which is dominant in terms of the inhibition of electron transfer and by how much.

We previously carried out photoaffinity labeling using a photoreactive analogue of natural acetogenin ([125 I]TDA, Figure 1). In this probe, as the phenyldiazirine ring acts as a mimic of the γ -lactone ring of natural products as well as a photoreactive functional group, the inhibitory effects of TDA on bovine complex I are identical to those of natural acetogenins (16). The photoaffinity labeling revealed that the residue cross-linked by the phenyldiazirine ring is located within the region of the fourth to fifth transmembrane helices (Val144–Glu192) of the ND1 subunit (17). Structure–activity studies for numerous acetogenins strongly suggested that the γ -lactone ring buries into the hydrophobic environment of the enzyme with the support of

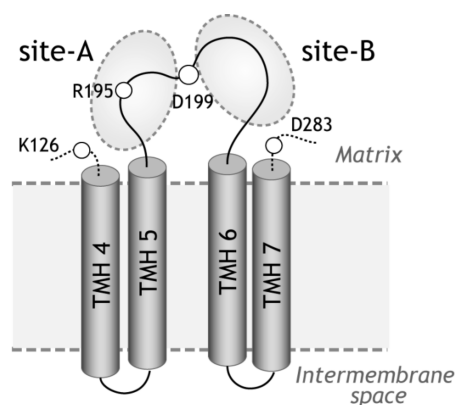


FIGURE 8: A hypothetical spatial arrangement of binding sites A and B in the membrane topology model of the ND1 subunit.

the hydrophobic alkyl spacer (27, 28). On the basis of these findings along with the present results, it is reasonable to consider that the amino acid residue cross-linked by the phenyldiazirine ring of [125 I]TDA resides in the hydrophobic fourth or fifth transmembrane helix. If so, site A may be the site which accommodates the hydroxylated bis-THF ring of natural acetogenins. This idea is in agreement with the above model; namely, the greater the occupation of site A, the greater the superoxide production. On the other hand, structure–activity studies for natural acetogenins also revealed that the hydroxylated bis-THF ring moiety is recognized by complex I in a fairly loose way (24–28); for instance, neither the number of THF rings nor the stereochemistry around the hydroxylated THF ring moiety is an essential factor for the inhibition. It is therefore not strange that the photoreactive diazirine group attached to the bis-THF ring cross-links with different amino acid residues at site A.

Furthermore, an excess amount of Δ lac-acetogenin (**2**) did not block the cross-linking of [125 I]DAA to site A (Figure 7). This result is consistent with the previous observation that the level of superoxide production induced by bullatacin was not affected in the presence of **2** at excess concentrations (see Figure 5 in ref 31). Thus, the results of the competition tests lead us to believe that the binding site of Δ lac-acetogenins may not overlap with that of natural acetogenins. The extremely efficient suppression of the

binding of [125 I]DAA to site B by bullatacin (Figure 4) may be due to a structural change at site B induced by bullatacin (i.e., an allosteric effect). Therefore, the results of the present study can be explained by assuming that the bis-THF ring moiety of natural acetogenins and Δ lac-acetogenins resides at site A and site B, respectively, in the third matrix side loop. Given that an excess of Q_2 predominantly blocked the binding of [125 I]DAA to site B (Figure 7C), this site may participate in the binding or the access path of ubiquinone to the "quinone cavity" which may be formed by the PSST and 49 kDa subunits (6).

Rotenone, piericidin A, and 6-aminoquinazoline completely suppressed the binding of [125 I]DAA to both sites A and B at higher concentration than that required for bullatacin (Figure 4). Our previous studies strongly suggested that the binding site of Δ lac-acetogenins might not overlap with that of the classical inhibitors (16, 30, 31). The suppression of the binding of [125 I]DAA to site B by the classical inhibitors may also be due to an allosteric effect. Solely from the competition test performed in the present study, it is hard to answer as to whether the suppression of the binding of [125 I]DAA to site A is due to true competitive behavior or allosteric effect. It remains to be learned how the binding positions of chemically diverse classical inhibitors are related to each other.

Elucidation of the mechanism of superoxide generation from complex I is critical for the formulation of causative connection between the enzyme defects and pathological effects. Most research groups working in the complex I field favor the idea that superoxide is primarily generated at the reduced FMN in isolated enzyme (53–56). However, it is difficult to unambiguously pinpoint the site of superoxide generation from complex I in intact mitochondria or SMP in the presence of "quinone-site inhibitors" (57, 58). There is some controversy about the presence of two separate sites in complex I (FMN and ubiquinone-binding site) rather than a single site (56, 59). We reproducibly confirmed that during the forward electron transfer, Δ lac-acetogenins induce superoxide generation from bovine complex I at a much lower rate than do classical inhibitors (30, 31). Now the binding site of these unique inhibitors appeared to reside in the membrane subunit ND1, which is located downstream of all the redox cofactors (FMN and iron–sulfur clusters) residing in the hydrophilic domain. Therefore, the present findings are of value for discussing the site of superoxide generation. When the reduction of ubiquinone in complex I is fully blocked by classical inhibitors or Δ lac-acetogenin, the extent to which electrons accumulate in a linear chain of the cofactors should be comparable (57, 58). Therefore, the difference in superoxide generation would not be attributable to a difference in the electron leak from the cofactors to molecular oxygen. It is most likely that the blocking effect of Δ lac-acetogenin on the reduction of ubiquinone causes less electron leak from ubisemiquinone to molecular oxygen than that of classical inhibitors. Considering that an excess of Q_2 completely blocked the binding of [125 I]DAA to site B, but not site A (Figure 7C), Δ lac-acetogenins may be a more effective competitor against ubiquinone than natural acetogenins and hence be better to reduce the formation of ubisemiquinone radical. Genova and colleagues (60) argued that the ubisemiquinone radical is not a candidate for a direct donor of electrons to molecular oxygen in the presence of a "quinone-site inhibitor" since the inhibitor remarkably diminished the formation of ubisemiquinone radical as revealed by EPR spectroscopy (61). However, one cannot exclude the possibility that a destabilized ubisemiquinone, perhaps undetectable by EPR under the

experimental conditions, and/or the residual ubisemiquinone serves as an electron donor to molecular oxygen (58, 62).

In conclusion, we synthesized a photoreactive Δ lac-acetogenin mimic, [125 I]DAA. Photoaffinity labeling using [125 I]DAA strongly suggested that the photo-cross-linked residues are located at two different sites, site A in the Ala135–Phe198 region and site B in the Asp199–Lys262 region, in the third matrix-side loop connecting the fifth and sixth transmembrane helices in the ND1 subunit. Site A and site B may be the site that accommodates the bis-THF ring moiety of natural acetogenins and Δ lac-acetogenins, respectively. Site B may contribute to the binding or the access path of ubiquinone to the "quinone cavity" formed by the PSST and 49 kDa subunits.

ACKNOWLEDGMENT

We thank Drs. Takahisa Kato and Hideo Miyatake (Radioisotope Research Center, Kyoto University) for technical assistance.

SUPPORTING INFORMATION AVAILABLE

Synthesis of DAA and [125 I]DAA and Figure S1. This material is available free of charge via the Internet at <http://pubs.acs.org>.

REFERENCES

- Walker, J. E. (1992) The NADH-ubiquinone oxidoreductase (complex I) of respiratory chains. *Q. Rev. Biophys.* 25, 253–324.
- Carroll, J., Fearnley, I. M., Skehel, J. M., Shannon, R. J., Hirst, J., and Walker, J. E. (2006) Bovine complex I is a complex of 45 different subunits. *J. Biol. Chem.* 281, 32724–32727.
- Sazanov, L. A., and Hinchliffe, P. (2006) Structure of the hydrophilic domain of respiratory complex I from *Thermus thermophilus*. *Science* 311, 1430–1436.
- Yagi, T., and Matsuno-Yagi, A. (2003) The proton-translocating NADH-quinone oxidoreductase in the respiratory chain: the secret unlocked. *Biochemistry* 42, 2266–2274.
- Brandt, U. (2006) Energy converting NADH:quinone oxidoreductase (complex I). *Annu. Rev. Biochem.* 75, 69–92.
- Sazanov, L. A. (2007) Respiratory complex I: mechanism and structural insights provided by the crystal structure of the hydrophilic domain. *Biochemistry* 46, 2275–2288.
- Friedrich, T., Van Heek, P., Leif, H., Ohnishi, T., Forche, E., Kunze, B., Jansen, R., Trowitzsch-Kienast, W., Höfle, G., Reichenbach, H., and Weiss, H. (1994) Two binding sites of inhibitors in NADH: ubiquinone oxidoreductase (complex I). *Eur. J. Biochem.* 219, 691–698.
- Degli Esposti, M. (1998) Inhibitors of NADH-ubiquinone reductase: an overview. *Biochim. Biophys. Acta* 1364, 222–235.
- Miyoshi, H. (1998) Structure-activity relationships of some complex I inhibitors. *Biochim. Biophys. Acta* 1364, 236–244.
- Heinrich, H., and Werner, S. (1992) Identification of the ubiquinone-binding site of NADH-ubiquinone oxidoreductase (complex I) from *Neurospora crassa*. *Biochemistry* 31, 11413–11419.
- Gong, X., Xie, T., Yu, L., Hesterberg, M., Scheide, D., Friedrich, T., and Yu, C.-A. (2003) The ubiquinone-binding site in NADH-ubiquinone oxidoreductase from *Escherichia coli*. *J. Biol. Chem.* 278, 25731–25737.
- Earley, F. G. P., and Ragan, C. I. (1984) Photoaffinity labeling of mitochondrial NADH dehydrogenase with arylazidoamorphigenin, an analogue of rotenone. *Biochem. J.* 224, 525–534.
- Earley, F. G. P., Patel, S. D., Ragan, C. I., and Attardi, G. (1987) Photolabeling of a mitochondrially encoded subunit of NADH dehydrogenase with [3 H]dihydrorotenone. *FEBS Lett.* 219, 108–113.
- Schuler, F., Yano, T., Bernardo, S. D., Yagi, T., Yankovskaya, V., Singer, T. P., and Casida, J. E. (1999) NADH-quinone oxidoreductase: PSST subunit couples electron transfer from iron-sulfur cluster N2 to quinone. *Proc. Natl. Acad. Sci. U.S.A.* 96, 4149–4153.
- Nakamaru-Ogiso, E., Sakamoto, K., Matsuno-Yagi, A., Miyoshi, H., and Yagi, T. (2003) The ND5 subunit was labeled by a photoaffinity analogue of fenpyroximate in bovine mitochondrial complex I. *Biochemistry* 42, 746–754.
- Murai, M., Ishihara, A., Nishioka, T., Yagi, T., and Miyoshi, H. (2007) The ND1 subunit constructs the inhibitor binding domain in bovine heart mitochondrial complex I. *Biochemistry* 46, 6409–6416.

17. Sekiguchi, K., Murai, M., and Miyoshi, H. (2009) Exploring the binding site of acetogenin in the ND1 subunit of bovine mitochondrial complex I. *Biochim. Biophys. Acta* 1781, 1106–1111.
18. Murai, M., Sekiguchi, K., Nishioka, T., and Miyoshi, H. (2009) Characterization of the inhibitor binding site in mitochondrial NADH-ubiquinone oxidoreductase by photoaffinity labeling using a quinazoline-type inhibitor. *Biochemistry* 48, 688–698.
19. Ahlers, P. M., Zwicker, K., Kersch, S., and Brandt, U. (2000) Function of conserved acidic residues in the PSST homologue of complex I (NADH-ubiquinone oxidoreductase) from *Yarrowia lipolytica*. *J. Biol. Chem.* 275, 23577–23582.
20. Kashani-Poor, N., Zwicker, K., Kersch, S., and Brandt, U. (2001) A central functional role for the 49-kDa subunit within the catalytic core of mitochondrial complex I. *J. Biol. Chem.* 276, 24082–24087.
21. Prieur, I., Lunardi, J., and Dupuis, A. (2001) Evidence for a quinone binding site close to the interface between NuoD and NuoB subunits of complex I. *Biochim. Biophys. Acta* 1504, 173–178.
22. Baranova, E. A., Holt, P. J., and Sazanov, L. A. (2007) Projection structure of the membrane domain of *Escherichia coli* respiratory complex I at 8 angstrom resolution. *J. Mol. Biol.* 366, 140–154.
23. Okun, J. G., Lümmen, P., and Brandt, U. (1999) Three classes of inhibitor share a common binding domain in mitochondrial complex I (NADH-ubiquinone oxidoreductase). *J. Biol. Chem.* 274, 2625–2630.
24. Miyoshi, H., Ohshima, M., Shimada, H., Akagi, T., Iwamura, H., and McLaughlin, J. L. (1998) Essential structural factors of *Annonaceous* acetogenins as potent inhibitors of mitochondrial complex I. *Biochim. Biophys. Acta* 1365, 443–452.
25. Motoyama, T., Yabunaka, H., and Miyoshi, H. (2002) Essential structural factors of acetogenins, potent inhibitors of mitochondrial complex I. *Bioorg. Med. Chem. Lett.* 12, 2089–2092.
26. Abe, M., Kenmochi, A., Ichimaru, N., Hamada, T., Nishioka, T., and Miyoshi, H. (2004) Essential structural features of acetogenins: role of hydroxy groups adjacent to the bis-THF rings. *Bioorg. Med. Chem. Lett.* 14, 779–782.
27. Abe, M., Murai, M., Ichimaru, N., Kenmochi, A., Yoshida, T., Kubo, A., Kimura, Y., Moroda, A., Makabe, H., Nishioka, T., and Miyoshi, H. (2005) Dynamic function of the alkyl spacer of acetogenins in their inhibitory action with mitochondrial complex I (NADH-ubiquinone oxidoreductase). *Biochemistry* 44, 14898–14906.
28. Abe, M., Kubo, A., Yamamoto, S., Hatoh, Y., Murai, M., Hattori, Y., Makabe, H., Nishioka, T., and Miyoshi, H. (2008) Dynamic function of the spacer region of acetogenins in the inhibition of bovine mitochondrial NADH-ubiquinone oxidoreductase (complex I). *Biochemistry* 47, 6260–6266.
29. Hamada, T., Ichimaru, N., Abe, M., Fujita, D., Kenmochi, A., Nishioka, T., Zwicker, K., Brandt, U., and Miyoshi, H. (2004) Synthesis and inhibitory action of novel acetogenin mimics with bovine heart mitochondrial complex I. *Biochemistry* 43, 3651–3658.
30. Ichimaru, N., Murai, M., Abe, M., Hamada, T., Yamada, Y., Makino, S., Nishioka, T., Makabe, H., Makino, A., Kobayashi, T., and Miyoshi, H. (2005) Synthesis and inhibition mechanism of Δ lac-acetogenins: a novel type of inhibitor of bovine heart mitochondrial complex I. *Biochemistry* 44, 816–825.
31. Murai, M., Ichimaru, N., Abe, M., Nishioka, T., and Miyoshi, H. (2006) Mode of inhibitory action of Δ lac-acetogenins, a new class of inhibitors of bovine heart mitochondrial complex I. *Biochemistry* 45, 9778–9787.
32. Belogradov, G. I., and Hatefi, Y. (1994) Catalytic sector of complex I (NADH-ubiquinone oxidoreductase): subunit stoichiometry and substrate-induced conformational changes. *Biochemistry* 33, 4571–4576.
33. Yamaguchi, M., Belogradov, G. I., and Hatefi, Y. (1998) Mitochondrial NADH-ubiquinone oxidoreductase (complex I): effects of substrates on the fragmentation of subunits by trypsin. *J. Biol. Chem.* 273, 8094–8098.
34. Mamedova, A. A., Holt, P. J., Carroll, J., and Sazanov, L. A. (2004) Substrate-induced conformational change in bacterial complex I. *J. Biol. Chem.* 279, 23830–23836.
35. Berrisford, J. M., Thompson, C. J., and Sazanov, L. A. (2008) Chemical and NADH-induced, ROS-dependent, cross-linking between subunits of complex I from *Escherichia coli* and *Thermus thermophilus*. *Biochemistry* 47, 10262–10270.
36. Ino, T., Nishioka, T., and Miyoshi, H. (2003) Characterization of inhibitor binding sites of mitochondrial complex I using fluorescent inhibitor. *Biochim. Biophys. Acta* 1605, 15–20.
37. Smith, A. L. (1967) Preparation, properties and conditions for assay of mitochondria: slaughterhouse material, small scale. *Methods Enzymol.* 10, 81–86.
38. Matsuno-Yagi, A., and Hatefi, Y. (1985) Studies on the mechanism of oxidative phosphorylation. *J. Biol. Chem.* 260, 14424–14427.
39. Ernster, L., and Lee, C.-P. (1967) Energy-linked reduction of NAD^+ by succinate. *Methods Enzymol.* 10, 729–738.
40. Boveris, A. (1984) Determination of the production of superoxide radicals and hydrogen peroxide in mitochondria. *Methods Enzymol.* 105, 429–435.
41. Laemmli, U. K. (1970) Cleavage of structural proteins during the assembly of the head of bacteriophage T4. *Nature* 227, 680–685.
42. Zerbetto, E., Vergani, L., and Dabbeni-Sala, F. (1997) Quantification of muscle mitochondrial oxidative phosphorylation enzymes via histochemical staining of blue native polyacrylamide gels. *Electrophoresis* 18, 2059–2064.
43. Wittig, I., Braun, H. P., and Schägger, H. (2006) Blue native PAGE. *Nat. Protoc.* 1, 418–428.
44. Sazanov, L. A., Peak-Chew, S. Y., Fearnley, I. M., and Walker, J. E. (2000) Resolution of the membrane domain of bovine complex I into subcomplexes: implications for structural organization of the enzyme. *Biochemistry* 39, 7229–7235.
45. Schägger, H. (2006) Tricine-SDS-PAGE. *Nat. Protoc.* 1, 16–21.
46. Ichimaru, N., Abe, M., Murai, M., Senoh, M., Nishioka, T., and Miyoshi, H. (2006) Function of the alkyl side chains of Δ lac-acetogenins in the inhibitory effect on mitochondrial complex I (NADH-ubiquinone oxidoreductase). *Bioorg. Med. Chem. Lett.* 16, 3555–3558.
47. Ichimaru, N., Yoshinaga, N., Nishioka, T., and Miyoshi, H. (2007) Effect of stereochemistry of Δ lac-acetogenins on the inhibition of mitochondrial complex I (NADH-ubiquinone oxidoreductase). *Tetrahedron* 63, 1127–1139.
48. Carroll, J., Fearnley, I. E., Shannon, R. J., Hirst, J., and Walker, J. E. (2003) Analysis of the subunit composition of complex I from bovine heart mitochondria. *Mol. Cell. Proteomics* 2, 117–126.
49. Valentino, M. L., Barboni, P., Ghelli, A., Bucci, L., Rengo, C., Achilli, A., Torroni, A., Liguori, A., Lodi, R., Barbiroli, B., Dotti, M. T., Federico, A., Baruzzi, A., and Carelli, V. (2004) The ND1 gene of complex I is a mutational hot spot for Leber's hereditary optic neuropathy. *Ann. Neurol.* 56, 631–641.
50. Kirby, D. M., McFarland, R., Ohtake, A., Dunning, C., Ryan, M. T., Wilson, C., Ketteridge, D., Turnbull, D. M., Thorburn, D. R., and Taylor, R. W. (2004) Mutations of the mitochondrial ND1 gene as a cause of MELAS. *J. Med. Genet.* 41, 784–789.
51. Sinha, P. K., Torres-Bacete, J., Nakamaru-Ogiso, E., Castro-Guerreo, N., Matsuno-Yagi, A., and Yagi, T. (2009) Critical roles of subunit NuoH (ND1) in the assembly of peripheral subunits with the membrane domain of *Escherichia coli* NDH-1. *J. Biol. Chem.* 284, 9814–9823.
52. Roth, R., and Hägerhäll, C. (2001) Transmembrane orientation and topology of the NADH:quinone oxidoreductase putative quinone binding subunit NuoH. *Biochim. Biophys. Acta* 1504, 352–362.
53. Liu, Y., Fiskum, G., and Schubert, D. (2002) Generation of reactive oxygen species by the mitochondrial electron transport chain. *J. Neurochem.* 80, 780–787.
54. Galkin, A., and Brandt, U. (2005) Superoxide radical formation by pure complex I (NADH:ubiquinone oxidoreductase) from *Yarrowia lipolytica*. *J. Biol. Chem.* 280, 30129–30135.
55. Kussmaul, L., and Hirst, J. (2006) The mechanism of superoxide production by NADH:ubiquinone oxidoreductase (complex I) from bovine heart mitochondria. *Proc. Natl. Acad. Sci. U.S.A.* 103, 7607–7612.
56. Hirst, J., King, M. S., and Pryde, K. R. (2008) The production of reactive oxygen species by complex I. *Biochem. Soc. Trans.* 36, 976–980.
57. Lambert, A. J., and Brand, M. D. (2004) Superoxide production by NADH:ubiquinone oxidoreductase (complex I) depends on the pH gradient across the mitochondrial inner membrane. *Biochem. J.* 382, 511–517.
58. Lambert, A. J., and Brand, M. D. (2004) Inhibitors of the quinone-binding site allow rapid superoxide production from mitochondrial NADH-ubiquinone oxidoreductase (complex I). *J. Biol. Chem.* 279, 39414–39420.
59. Brand, M. D. (2010) The sites and topology of mitochondrial superoxide production. *Exp. Gerontol.* (doi: 10.1016/j.exger.2010.01.003).
60. Genova, M. L., Ventura, B., Giuliano, G., Bovine, C., Formiggin, G., Castelli, G. P., and Lenaz, G. (2001) The site of production of superoxide radical in mitochondrial complex I is not a bound ubiquinone but presumably iron-sulfur cluster N2. *FEBS Lett.* 505, 364–368.
61. Burbaev, D. S., Moroz, I. A., Kotlyar, A. B., Sled, V. D., and Vinogradov, A. D. (1989) Ubisemiquinone in the NADH-ubiquinone reductase region of the mitochondrial respiratory chain. *FEBS Lett.* 254, 47–51.
62. Ohnishi, S. T., Ohnishi, T., Muranaka, S., Fujita, H., Kimura, H., Umura, K., Yoshida, K., and Utsumi, K. (2005) A possible site of superoxide generation in the complex I segment of rat heart mitochondria. *J. Bioenerg. Biomembr.* 37, 1–15.